Study of bioactivity, biodegradability and mechanical properties of polyurethane/nano-hydroxyapatite hybrid composites

A.B. Martínez-Valencia, G. Carbajal-De la Torre, A. Duarte Moller, H.E. Esparza-Ponce and M.A. Espinosa-Medina

Abstract

The present research is focused on the study of a series of polyurethane/nano-hydroxyapatite composites with different nano-hydroxyapatite (nHA) compositions (0, 10, 20, 30 and 40 %wt). Mechanical, biodegradability and bioactivity properties of composites were evaluated. Tensile tests were performed using a dynamic mechanical analyzer (DMA). Biodegradability and bioactivity studies were done by immersion into phosphate buffered saline (PBS) and simulated body fluid (SBF) solutions respectively. Both biodegradability and bioactivity behavior of specimens were monitored by gravimetric method and morphologically characterized by Scanning Electron Microscopy (SEM). Mechanical test results showed that both pure polyurethane and the 10 wt% nHA composite presented similar Young's modulus of 4.4 and 4.7 MPa, respectively. On the other hand, at higher nHA contents, the composites became relatively brittle showing Young's modulus from 6.6 to 8.3 MPa values. The biodegradation rate increased as a function of nHA contents. In that way, polyurethane and composite containing 10 and 40 wt% nano-hydroxyapatite lost weight about 3 and 4wt%, respectively during 56 days of immersion. Study of bioactivity revealed that the composites exhibits advantages compared with polyurethane. The formation of bone-like apatite microstructure was corroborated by X-Ray Diffraction (XRD), Fourier

transformed infrared spectroscopy (FTIR) and Scanning Electron Microscopy (SEM) coupled energy dispersive X-ray (EDS) analysis.

Key words: Polyurethane, nano-hydroxyapatite, biodegradability, bioactivity, mechanical properties.

Introduction

During the last two decades, polymer/bioactive ceramic composite materials have been extensively developed for tissue engineering applications such as bone tissue regeneration (Ramakrishna et al., 2001). Different polymer/calcium phosphate composites for bone replace-ment and tissue regeneration applications were studied, trying to improve their mechanical properties in addition to their bioactivity, biodegradability and biocompatibility properties (Thein-Han et al., 2009; Liu et al., 2009; Biossard et al., 2009; Laschke et al., 2010; Jayabalan et al., 2010). In this sense, Ren et al. (2007) studied some poly (D,L-lactide)/ nano-hydroxyapatite (nHA) composites produced by *in-situ* polymerization of nHA and lactide monomer (2 and 4 wt.%); those composites presented high porosity but better hydrophilic capacity, mechanical properties improvement and excellent biocompatibility. Zhao et al. (2008) reported a highly porous hydroxiapatite (HA)/polycaprolactone composite scaffold with inter-connected porosity, superior mechanical and bioactive properties became a bone substitute option for clinical applications. Dong et al. (2009) reported that (30 wt%) nHA/PU composites scaffold presented good biocompatibility and bioactivity response, additionally both in vitro and in vivo biological test results showed that the nHA/PU scaffold was non-cytotoxic and degradable.

Biocomposites based in polyurethane (PU) with hydroxyapatite (HA) contents have been studied; however, hybrid composites and its HA wt.% contents effect have not been widely studied. Synthetic HA [$Ca_{10}(PO_4)_6(OH)$], has been the most suitable ceramic material for bone tissue replacement implants due mainly to biocompatibility, bioactivity and to the influence of the composite degradation rate, also improving mechanical properties (Suchanek and Yoshimura, 1998). Biodegrad-able PU is a more useful polymer kind as structural ele-ment for medical devices, showing excellent mechanical properties and good biocompatibility (Vermette and Griesser, 2001).

Considering the material qualities (nHA and PU) and their extensive medical applications, as reported (Martinez-Valencia et al., 2011), in this work, mechanical, biodegradation and bioactivity evaluations of PU/nHA hybrid composites and nHA contents effect was done. Results were complemented by XRD, FTIR and SEM coupled EDS analysis.

Material and method

Synthesis of PU/nHA composites

The starting nHA powders were synthesized by ultrasound-assisted coprecipitation wet chemical method as described previously (Martínez-Valencia et al., 2008). The obtained nHA powders presented micrometric and mesoporous nanocrystalline hydroxyapatite particle (*Dc*<40 nm) aggregates, showing high superficial area values (97.9 m^2g^{-1}) and homogeneous chemical composition. Then, obtained nHA powders were mixed with pure PU during the polymerization at different weight ratios: 0, 10, 20, 30 and 40 wt.%. The following reactants were used in polyurethane and composite synthesis: 1,6-diisocyanato hexane (HDI); polycaprolactone (PCL) and 1,4-

butanodiol (BD). The PU and composites were synthesized in bulk by a two-step solution polymerization method, as described previously (Martinez-Valencia et al., 2011). The reaction stoichiometry was 3:2:1 of HDI: PCL: BD.

Composite characterization

Mechanical characterization

Tensile tests were done by dynamic mechanical analyzer (DMA) using a RSA3 TA Instruments System. Composites with different compositions were formed by metallic mold deposition and compression at 65°C, applying 1.46 kg/cm^2 pressure for 3 min. Therefore, sheets of 50.0 mm length, 5 mm width and 0.15 mm thickness approximately were obtained. Tension tests were developed at room temperature (25°C) and 37°C (physiologic temperature) applying a 0.001 mm/s loading rate. That small strain rate test was selected considering an expected lower composite Young's modulus and the load was applied until the composite failed. For tension test, at least four samples of each composition were evaluated and the results were averaged. Young's modulus (E) and both ultimate tensile strength (σ) and elongation at failure (ε) were calculated from tension-strained curves.

Composite degradation

To measure composite hydrolytic degradation (according to ASTM F1635), small polyurethane, nHA specimens and composites were cut to obtain 8 mm diameter and 2 mm thick discs in order to perform an *in vitro* degradation study. All samples of each material were weighed with a high resolution micro-balance (±0.0001 mg), and immersed into an inert bottle with 30 ml of 0.01 M phosphate buffered saline (PBS) solution (PBS, pH = 7.4) and placed in an oven at 37 ±1°C at time periods of 1 to 8

weeks. Buffer solution was prepared with 0.138 M sodium chloride (NaCl) and 0.0027 M of potassium chloride (KCl) in 1 L of deionized water. The buffer was replaced frequently to ensure a constant pH of 7.4±0.05 value. Additional pH changes of PBS medium were measured at pre-set time intervals (0 to 7 days) using a pH-meter. At set up times, the composites were taken out of the buffer solution container, washing it with distilled water in order to remove saline solution, and then dried, weighed and kept in a desiccator for several days; then the remaining weight was calculated as:

$$\text{Remaining weight (\%)} = (W2 / W1) \times 100 \quad (1)$$

where W_1 and W_2 is the composite weight before and after degradation, respectively. Three samples of each composition were tested for each time interval and standard deviations were calculated.

Composite bioactivity

The specimens used for the bioactivity study had the same size described previously (8 mm diameter and 2 mm thickness discs). The simulated body fluid (SBF) used in the present study consisted of: NaCl, sodium hydrogen carbonate ($NaHCO_3$), KCl, di-potassium hydrogen phosphate trihydrate ($K_2HPO_4.3H_2O$), magnesium chloride hexahydrate ($MgCl_2.6H_2O$), calcium chloride ($CaCl_2$), sodium sulfate (Na_2SO_4), Tris-hydroxymethyl aminomethane: ($(HOCH_2)3CNH_2$) (Tris) per liter, as described by Kokubo and Takadama (2006). Composites were sterilized using an autoclave, followed by immersion of each specimen into 30 ml of SBF medium of pH 7.4 in a water bath maintained at 37±1°C for 4 weeks and the SBF was changed every day to freshly prepared buffer ensuring adequate ion concentration. After immersion for 1, 7, 14, and 21 days, the SBF immersion was interrupted and the specimens were washed with

distilled water to remove soluble inorganic ions. Later the specimens were dried and kept in a desiccator at room temperature for 24 h prior weighing and further examination. Composite mass increase during immersion in SBF was calculated using Equation (2)

$$\text{Mass increase (\%)} = (W_2 - W_1 / W_1) \times 100 \quad (2)$$

where W_1 and W_2 is composite weight before and after SBF immersion, respectively.

X-ray diffraction

The composition of products formed or deposited (as HA phase) on the surface composites post-immersion in SBF was evaluated by X-ray diffraction (XRD) analysis with a diffractometer model Bruker D8 Advance. Diffraction patterns were acquired ranging from 10 to 55° in 2θ at a scanning rate of 0.2°/min using the $K\alpha_{Cu}$.

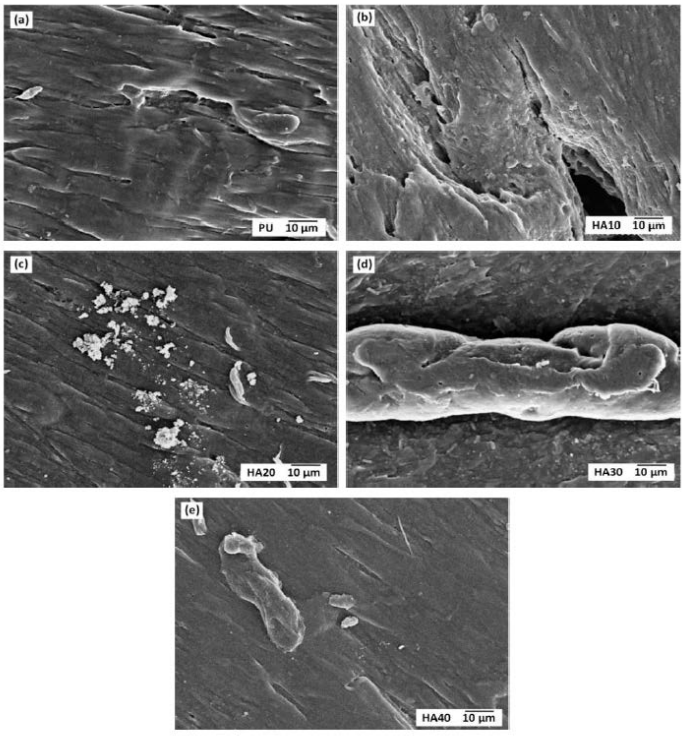

Figure 1. Secondary electron images (SEI) of PU and composites before analysis.

Fourier transformed infrared spectroscopy (FTIR)

Post-immersion in SBF infrared spectra composite analysis was performed in order to identify the characteristic functional groups corresponding to the HA formed on surface composites and were collected using a FTIR spectrophotometer (Bruker-Tensor 27). Each sample was scanned at a $1cm^{-1}$ resolution over the frequency range of 4000 to 400 cm^{-1}.

Morphology characterization

Scanning electron microscope (SEM) JEOL model JSM 6400, was used to characterize composite surface morphologies before and after immersion into the PBS and SBF solutions. Samples were finely sputter-coated with a copper thin film to ensure conductivity in the surface. SEM conditions for secondary electrons used were: 15 kV beam intensity acquiring low and high magnifications (1,000x and 10,000x). For elemental analysis in degraded composite surfaces and in order to verify the presence of calcium and phosphorus deposits on the sample surfaces analysis by energy dispersive X-ray spectroscopy (EDS) was performed.

Results and discussion

Since the combination of biodegradable polymers and inorganic bioactive particles represents the best approach in terms of possible mechanical and biological performance (Boccaccini and Gough 2007), biodegradable and bioactive PU/nHA composites were synthesized for their possible implementation as bone substitute. PU was synthesized based upon a PCL soft segment, an HDI hard segment and chain extension with BD. The nHA was prepared by mixing the corresponding quantities of calcium nitrate tetrahydrate [$Ca(NO_3).4H_2O$] and diammonium hydrogen phosphate [$(NH_4)_2HPO_4$], and a two-step polymerization solution was chosen as the method to

synthesize PU and PU/nHA materials with homogeneous composition. Samples were named as follows: The one containing 0%wt of nHA was labeled as (PU), the one containing 10%wt of nHA as (HA10), and 20% wt of nHA as (HA20) and so on.

Figure 1 shows PU morphologies and composites before immersion tests which were taken to examine nHA distribution in PU additionally. Results showed homogeneous nHA particle distribution within PU, in addition there were no visible areas of particle agglomerations found.

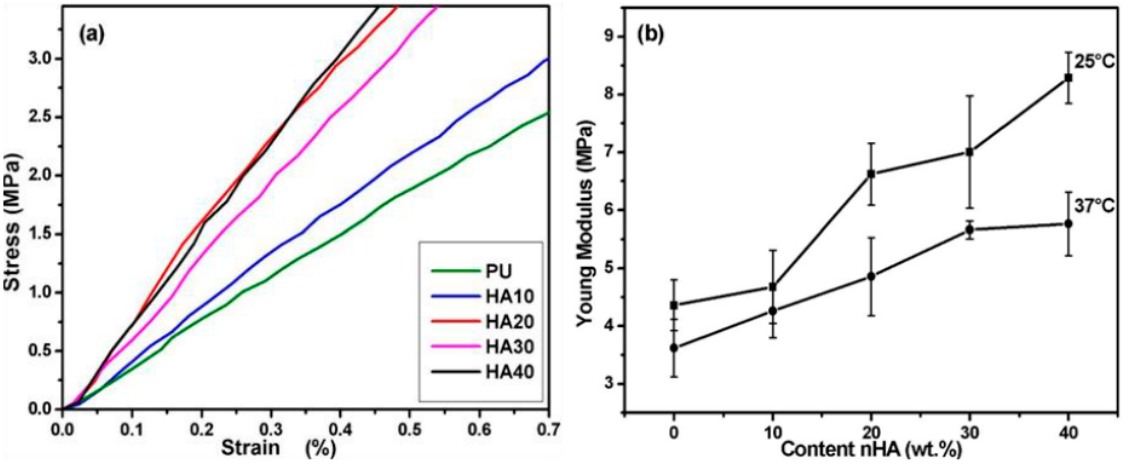

Figure 2. Representative stress–strain curves for PU and PU/nHA composites and Young's module as a function of the content nHA.

Table 1. Young's modulus of PU and composites.

Sample	Young's modulus (MPa), E	
	25°C	37°C
PU	4.36	3.62
HA10	4.68	4.26
HA20	6.62	4.86
HA30	7.00	5.72
HA40	8.29	5.76

Composite mechanical properties

Viscoelasticity is a feature of polymeric materials, and dynamic mechanical thermal analysis is one of the foremost tools for measuring polymer and polymer based nanocomposite viscoelasticity (Khan et al., 2009). The tensile test of pure PU and the four types of PU/nHA composites are shown in Figure 2. Figure 2a shows zoom area of tensile stress–strain curves used to determine mechanical properties for PU and PU/nHA composites, and the results of Young's modulus as a function of nHA mass fraction are shown in Figure 2b. The parameters from the stress–strain data at 25 and 37°C are summarized in Table 1. Composites with 20, 30 and 40% nHA concentrations presented hardness and fragile behavior showing fragmentation with hand manipulation, while PU and 10wt.% nHA composite showed the softest and most elastic characteristics. Comparing PU with 10wt.% nHA composite; did not show significant difference in keeping viscoelastic property. Results showed that Young's modulus increased from 4.36 to 8.29 MPa at 25°C and from 3.62 to 5.76 MPa at 37°C; additionally the Youngs modulus was higher by increasing amount of nHA, which HA40 composite presented the highest Young's modulus while the HA10 had the lowest. Those module values were acceptable compared with other results (Boissard et al., 2009). In general, Young's modulus of composites was higher than the ones presented by pure PU; moreover, the modulus also could increase as the particle size of nHA decreased, due to the higher dispersion probability in polymer matrix.

***In vitro* degradation**

The test method of in vitro degradation for PBS used in this work is about hydrolytically degradable polymers proposed for use in surgical implants. Degradation

analysis was performed to determine composite characteristics and degradation rate. Several time periods were set in order to obtain kinetic measurements. Figure 3 shows the mass remaining curves of pure nHA and PU/nHA composites versus incubation time. The data are expressed as the average of the three samples ± standard deviation. Results showed that all materials lost weight; nevertheless they show minimal degradation after an 8 weeks period of soaking immersion in PBS. A small rate increasing was presented between days 14 and 21 and the amount of mass loss was dependent on the material composition; the maximum degradation was showed for pure nHA (5% weight lost). Additionally, composites degraded faster to higher nHA percent (HA30 and HA40) as expected; HA10 and HA20 composites lost 3% from the initial mass after 8 weeks of immersion, while HA20 composite showed lower weight change.

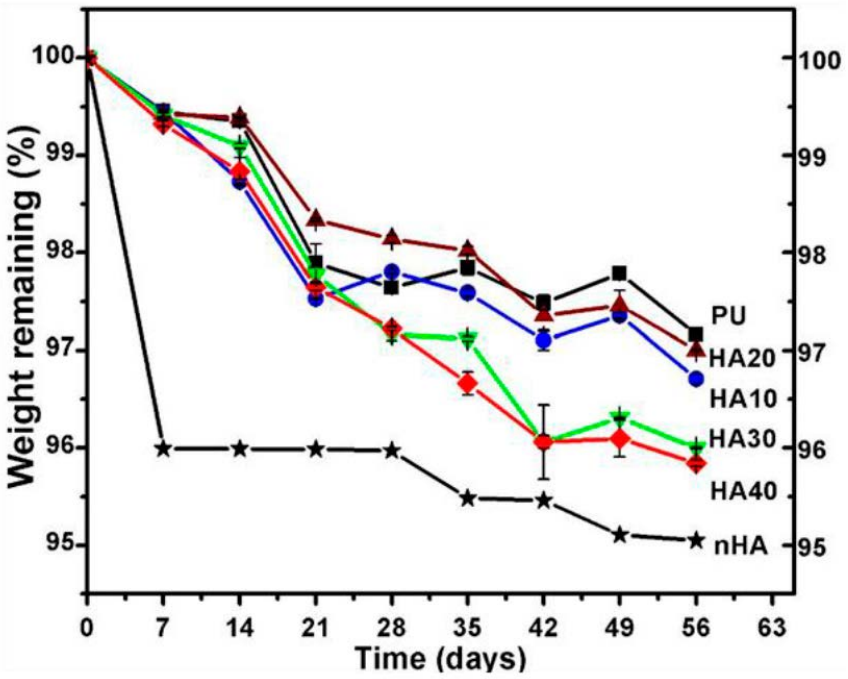

Figure 3. Incubation time of PU and composites in PBS solution versus weight remaining.

Figure 4 shows the surface materials post-immersion in PBS obtained by SEM. Characterization results showed more porosity and a little degree of surface cracking,

which increased with immersion time although the form and density of dissolution depend on the composition; that involves a possibility to increase or decrease composites dissolution susceptibility varying nHA amount and particle size.

***In vitro* bioactivity properties**

The ability to form a bone-like apatite onto the material surfaces were examined in SBF. That analysis is useful for predicting *in vivo* bone bioactivity both qualitatively and quantitatively. In addition, using this method can help predict material bioactive reactions before *in vivo* testing and as a result of this, the number of animals used and test duration could be minimized.

Figure 5 shows the weight increase curves of nHA and composites versus incubation time. Results showed that most composites presented a weight increase due to apatite formation until 15 days of immersion, while PU lost weight approximately 1%. In 21 days of immersion, all composites showed a differential weight decreasing probably due to the HA dilution in the SBF medium.

Evidence for weight changes due HA growing was obtained by XRD analysis. Figure 6a shows the XRD composite patterns at 7 days of immersion. Results confirm that the obtained phase was crystalline hydroxyapatite and secondary phases were not present. The presence of HA growing on the composites was supported from FTIR analysis. IR spectra for PU, nHA powder and HA40 composite at 7 days of immersion in SBF are presented in Figure 6b where all characteristic bands were observed. For PU principal bands of C-O at 1732 cm^{-1}, N-H stretching vibration at 3440 cm^{-1}, asymmetric and symmetric CH_2 stretching at 2945 and 2868 cm^{-1}, respectively were observed. For HA bands identified at 1033, 1095, 565 and 603 cm_{-1} correspond to PO_4^{3-} groups;

bands assigned to hydroxyl groups (OH^-) at 472 cm^{-1} confirmed the presence of HA phase. Stretching vibration at 3573 cm−1 of OH− was not observed from the composites which would suggest a bonding formation between composite PU and nHA formed.

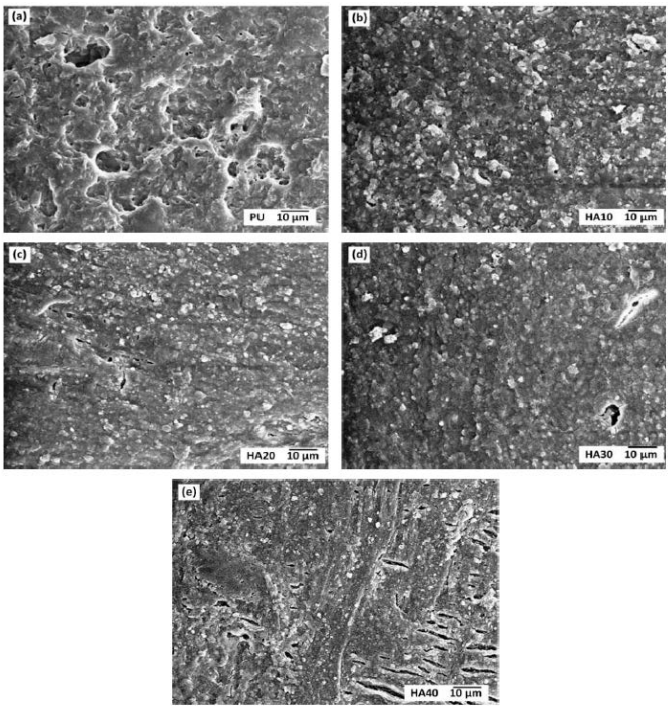

Figure 4. Images by SEM of surface composites post-immersion for 8 weeks in PBS: PU, 10, 20, 30 and 40 HA.

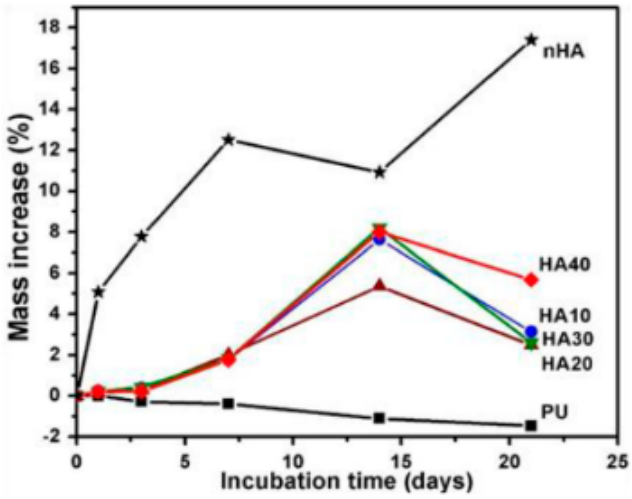

Figure 5. Mass increases of nHA and composites due to incubation time in SBF.

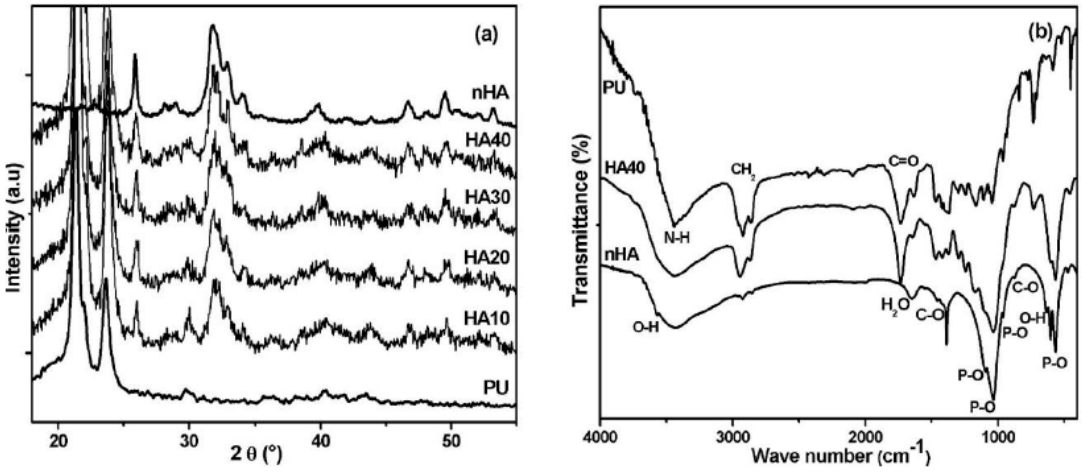

Figure 6. XRD pattern and FT-IR spectra of PU, nHA and composites immersed in SBF for 7 days.

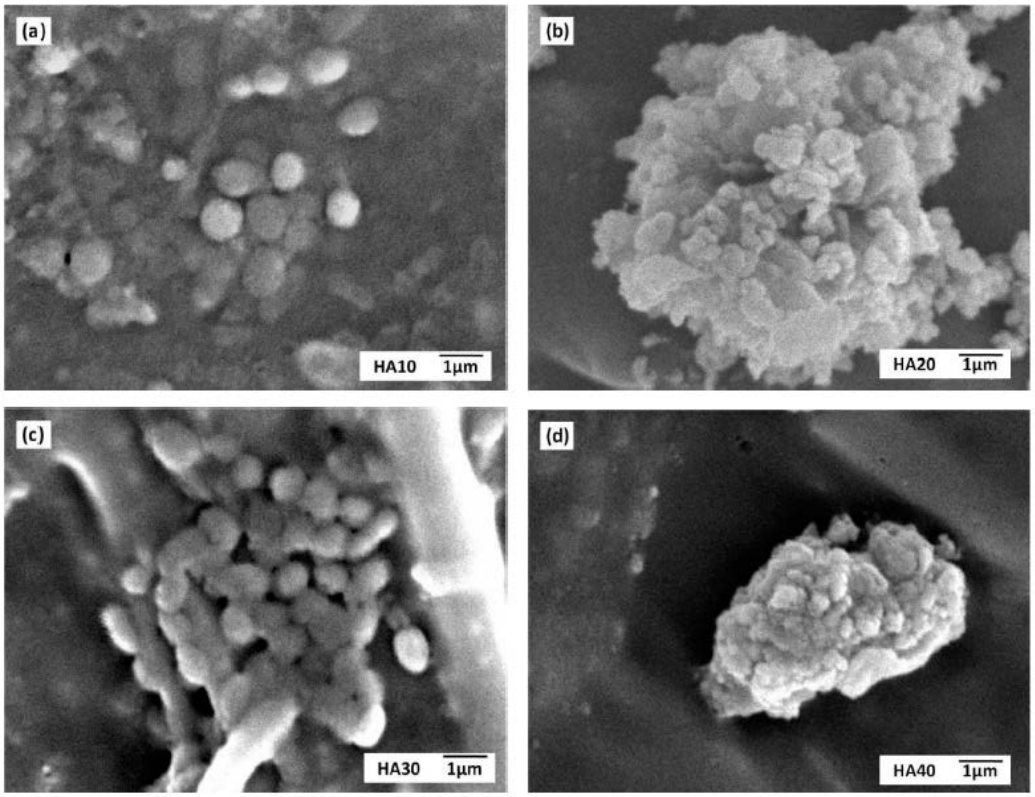

Figure 7. SEM micrographs of composites PU/nHA post-immersion during one day in SBF.

In Figures 7 to 10, SEM composite surface images are observed after different immersion times. Results showed that the materials were capable of forming spheric shaped apatite on the surface, in all cases it happened in a short time period, having

high capacity bonds to living bone in a short time period. Figure 7 shows the sample surface after one day of immersion which observed spherical particles less than 1 μm. Similarly, at 7 days of immersion, the size of the spherical particles increases by forming agglomerates observed with time increases, which were accumulating in order to form a compact layer (Figure 8).

Figure 9 presents the gradual development of HA on the surface as a result of increasing immersion time (14 days). At that immersion time, all specimens were covered by compacted product layers of HA showing cracking that was attributed to scale dehydration after drying; similarly, at 21 days of immersion, composites kept in the incubator, apatite showed similar size and shape as shown in Figure 10. In addition, apatite layer formation proves that the increase of nHA content into composite improved the apatite layer spherical shape size, compared to other composites (Dong et al., 2009; Liu et al., 2009).

Composite surface deposition by SBF reactions was analyzed semi-quantitatively by EDS. Results showed that the surface contained calcium (Ca) and phosphorous (P) elements. HA detected at one day of immersion presented a Ca/P mean average ratio of about 1.5, while at the first week post-immersion, the Ca/P mean ratio was approximately 1.85. After 14 days of immersion, all surfaces were completely covered by a compact layer of HA and Ca/P with mean average ratio of about 1.6 nearby to 1.67 corresponding to stoichiometric hydroxyapatite. The Ca/P mean ratio measured on the surfaces was observed at 21 days keeping stable. In Figure 11 are showed the EDS results before and after immersion of HA40 composite at 21 days. These results

showed an increase in both calcium and phosphorus signal as a result of the growth of HA.

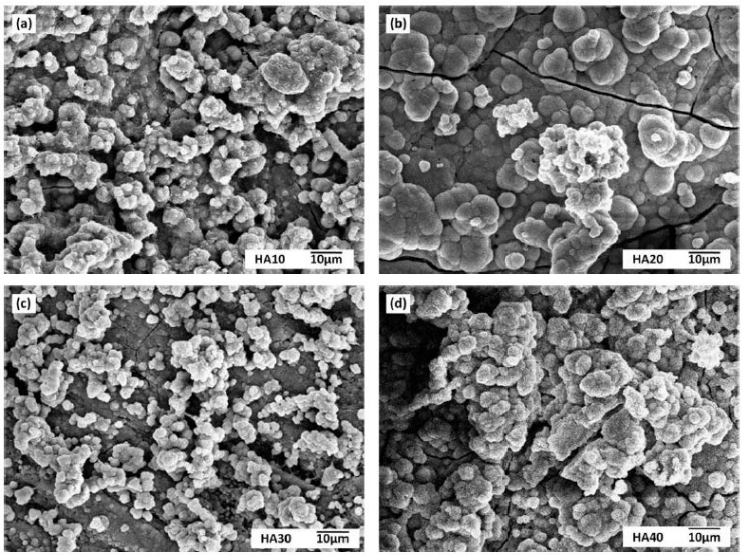

Figure 8. SEM micrographs of PU/nHA composites post-immersion to 7 days in SBF.

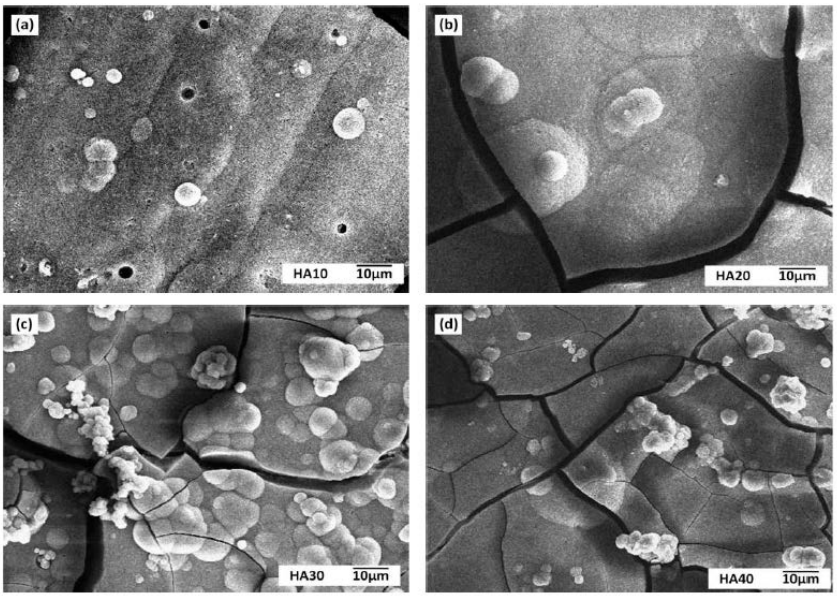

Figure 9. SEM micrographs of PU/nHA composites post-immersion to 14 days in SBF.

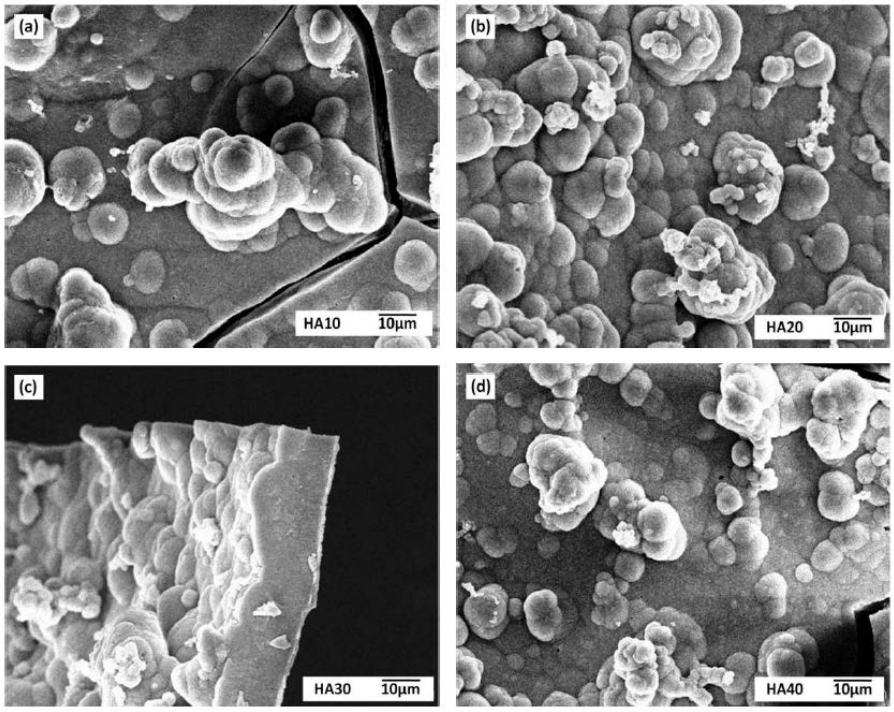

Figure 10. SEM micrographs of PU/nHA composites post-immersion to 21 days in SBF.

Conclusions

According to the results, PU/nHA composite synthesis using a two-step polymerization method is feasible for synthesized nanocomposites with homogeneous composition.

Composites showed satisfactory mechanical properties giving the possibility for using them as both structural substitute and regeneration element of bones in future applications, particularly, the 10 and 20 wt.% composites due to low biodegradability and acceptable elastic module.

In addition, results confirmed as well that all the composites have high ability to form an apatite layer on their surfaces; especially composites with high nHA contents increased apatite formation growing. Each of these composites has its distinctive

characteristics and could be studied under *in vivo* conditions in the future for specific medical applications.

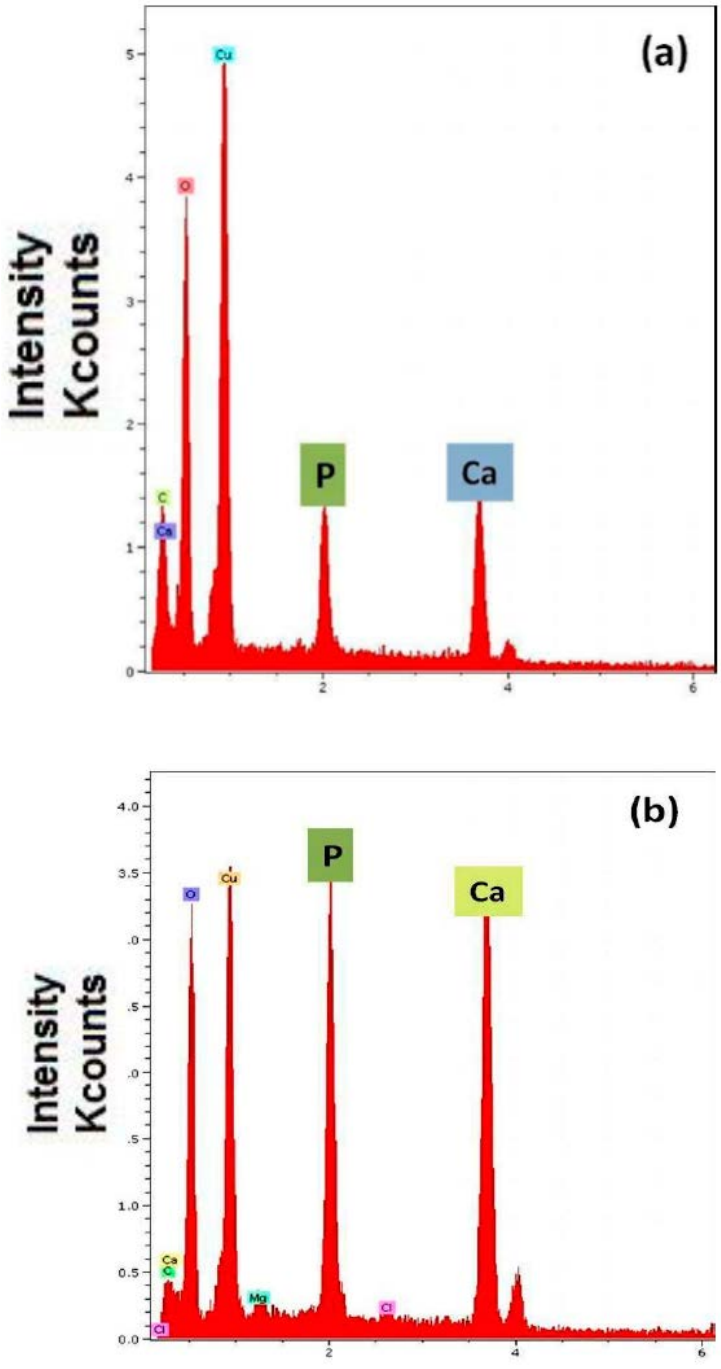

Figure 11. EDS before (a) and after (b) immersion in SBF HA40 composite.

Acknowledgements

We acknowledge the financial support from CONACYT from which A. B. Martinez-Valencia is fellow, as well as UMNSH-PTC-227 for financial support. The authors wish to thank M. Mendoza D., E. López M. for their technical support in the mechanical properties with DMA.

References

Boccaccini AR, Gough JE (2007). Tissue engineering using ceramics and polymers. Woodhead-publishing, pp. 72-89.

Boissard CIR, Bourban PE, Tami AE, Alini M, Eglin D (2009). Nanohydroxyapatite/poly(ester urethane) scaffold for bone tissue engineering. Acta. Biomater., 5: 3316-3327.

Dong Z, Li Y, Zou Q (2009). Degradation and biocompatibility of porous nano-hydroxyapatite/polyurethane composite scaffold for bone tissue engineering. Appl. Surf. Sci., 255: 6087-6091.

Jayabalan M, Shalumon KT, Mitha MK, Ganesan K, Epple M (2010). Effect of hydroxyapatite on the biodegradation and biomechanical stability of polyester nanocomposites for orthopedic applications. Act. Biomater., 6: 763–775.

Khan A, Shamsi MH, Choi TS (2009). Correlating dynamical mechanical properties with temperature and clay composition of polymer-clay nanocomposites. Comp. Mater. Sci., 45: 257-265.

Kokubo T, Takadama H (2006). How useful is SBF in predicting *in vivo* bone bioactivity? Biomaterials, 27: 2907-2915.

Liu X, Smith LA, Hu J, Ma PX (2009). Biomimetic nanofibrous gelatin/apatite composite scaffolds for bone tissue engineering. Biomaterials, 30: 2252–2258. Laschke MW,

Strohe A, Menger MD, Alini M, Eglin D (2010). *In vitro* and in vivo evaluation of a novel nanosize hydroxyapatite particles/poly(ester-urethane) composite scaffold for bone tissue engineering. Acta. Biomater., 6: 2020-2027.

Martínez-Valencia AB, Esparza-Ponce HE, Carbajal-De la Torre G, Ortiz-Landeros J (2008). Morphological and structural characterization of nanostructured of nanostrutured hydroxyapatite: Comparative study of different methods of synthesis. Surf. Vacuum., 21(4): 18-21.

Martinez-Valencia AB, Carbajal-De la Torre G, Torres-Sánchez R, Téllez-Jurado L, Esparza-Ponce HE (2011). Production of polyurethane/ nano-hydroxyapatite hybrid materials and microstructural characterization. Int. J. Phys. Sci., 6(11): 2731-2743.

Ramakrishna S, Mayer J, Wintermantel E, Leong KW (2001). Biomedical applications of polymer-composite materials: a review. Compos. Sci. Technol., 61: 1189-1224.

Ren J, Zhao P, Ren T, Gu S, Pan K (2007). Poly (D,L-lactide)/nano-hydroxyapatite composite scaffolds for bone tissue engineering and biocompatibility evaluation. J. Mater. Sci-Mater Med., 19: 1075-1082.

Suchanek W, Yoshimura M (1998). Processing and properties of hydroxyapatite-based biomaterials \for use as hard tissue replacement implants. J. Mater. Res., 13: 94-117.

Thein-Han WW, Shah J, Misra RDK (2009). Superior in vitro biological response and mechanical properties of an implantable nanostructured biomaterial: nanohydroxyapatite/silicone rubber composite. Acta. Biomater., 5: 2668-2679.

Vermette P, Griesser HJ (2001). Biomedical Applications of Polyurethanes. CSIRO Mol. Sci., pp. 77-91.

Zhao J, Guo LY, Yang XB, Weng J (2008). Preparation of bioactive porous HA/PCL composite scaffolds. Appl. Surf. Sci., 255: 2942- 2946.